Inorg. Chem. **2005**, *44*, 8670–8679

Intermetallic Compounds with Near Zintl Phase Behavior: $RE_2Zn_3Ge_6$ (RE = La, Ce, Pr, Nd) Grown from Liquid Indium

James R. Salvador,[†] Daniel Bilc,[‡] Jeffrey R. Gour,[†] Subhendra D. Mahanti,[‡] and Mercouri G. Kanatzidis*,[†]

Departments of Chemistry and Physics and Astronomy, Michigan State University, East Lansing, Michigan 48842

Received June 10, 2005

A series of compounds has been discovered while investigating reactions of rare earth, transition metals, and Ge in excess indium. These compounds, $RE_2Zn_3Ge_6$ (RE = La, Ce, Pr, Nd), are isostructural, crystallizing in the orthorhombic space group C*mcm* with lattice parameters $a = 5.9691(9)$ Å, $b = 24.987(4)$ Å, and $c = 5.9575(9)$ Å for $La_2Zn_3Ge_6$, $a = 5.9503(5)$ Å, $b = 24.761(2)$ Å, and $c = 5.9477(5)$ Å for the Ce analogue, $a = 5.938(2)$ Å, $b = 24.708(8)$ Å, and $c = 5.936(2)$ Å for $Pr_2Zn_3Ge_6$, and $a = 5.9094(7)$ Å, $b = 24.619(3)$ Å, and $c = 5.9063(5)$ Å for the Nd analogue. The structure is composed of PbO-like ZnGe layers and $ZnGe_4$ cage layers and is related to the $Ce_4Zn_8Ge_{11-x}$ structure type. The bonding in the system can be rationalized using the Zintl concept resulting in a material that is expected to be a valence precise semiconductor, although its behavior is more consistent with it being a semimetal, making it an intermediate case. The results of band structure calculations and magnetic measurements of these compounds are discussed.

Introduction

The remarkable utility of Al and Ga as solvents to explore new intermetallic phases in the systems RE/TM/Al,[1] RE/TM/Al/Si(Ge),[2] RE/TM/Ga/Si(Ge)[3], RE/TM/Ga, and RE/Ga/Ge (RE is a rare earth metal and TM is a transition metal) has facilitated the discovery of many new and novel materials. These include Sm_2NiGa_{12},[4] $Eu_4Ga_8Ge_{16}$,[5] $Ba_8Ga_{16}Ge_{30}$,[6] and $Yb_3Ga_6Ge_4$.[7] This raises the question as to how indium would perform. Indium possesses many of the same qualities that make Al and Ga attractive for exploratory synthesis, namely, its low melting point, its inability to form binaries with Ge or Si, and the solubility of Ge, Si, and a host of transition and lanthanide metals in it.[8] It is therefore a logical candidate to use in the extension of the work listed above to systems such as RE/TM/Ge/In. Studies have been published by several groups describing the use of molten In as a method to grow large single crystals of RE/TM/Ge compounds to investigate their physical properties more carefully,[9] although much less work has been done using In as a medium for exploratory synthesis.[10]

We have recently demonstrated the ability of liquid indium to stabilize a new form of the compound $RENiGe_2$ (RE = Dy, Er, Tm, Yb, Lu) which could not be made by direct combination of the elements and was exclusive to the In

* To whom correspondence should be addressed. E-mail: kanatzid@cem.msu.edu.
† Department of Chemistry.
‡ Department of Physics and Astronomy.

(1) (a) Fehrmann, B.; Jeitschko, W. *Inorg. Chem.* **1999**, *38*, 3344. (b) Fehrmann, B.; Jeitschko, W. *Z. Naturforsch. B* **1999**, *54*, 1277. (c) Fehrmann, B.; Jeitschko, W. *J. Alloys Compnds.* **2000**, *298*, 153. (d) Niermann, J.; Fehrmann, B.; Wolff, M. W.; Jeitschko, W. *J. Solid State Chem.* **2004**, *177*, 2600.
(2) (a) Sieve, B.; Trikalitis, P. N.; Kanatzidis M. G. *Z. Anorg. Allg. Chem.* **2002**, *628*, 1568. (b) Sieve, B.; Sportouch, S.; Chen, X.-Z.; Cowen, J. A.; Brazis, P.; Kannewurf, C. R.; Papaefthymiou, V.; Kanatzidis, M. G. *Chem. Mater.* **2001**, *13*, 273. (c) Latturner, S. E.; Bilc, D.; Mahanti, S. D.; Kanatzidis, M. G. *Chem. Mater.* **2002**, *14*, 1695.
(3) Zhuravleva, M. A.; Chen, X.-Z.; Wang, X. P.; Schultz, A. J.; Ireland, J.; Kannewurf, C. R.; Kanatzidis, M. G. *Chem. Mater.* **2002**, *14*, 3066.
(4) Chen, X.-Z.; Small, P.; Sportouch, S.; Zhuravleva, M.; Brazis, P.; Kannewurf, C. R.; Kanatzidis, M. G. *Chem. Mater.* **2000**, *12*, 2520.
(5) Bryan, D.; Stucky, G. D. *Chem. Mater.* **2001**, *13*, 253.
(6) Latturner, S. E.; Bryan, J. D.; Blake, N.; Metiu, H.; Stucky, G. D. *Inorg. Chem.* **2002**, *41*, 3956.
(7) Zhuravleva, M. A.; Salvador, J. R.; Bilc, D.; Mahanti, S. D.; Ireland, J.; Kannewurf, C. R.; Kanatzidis, M. G. *Chem. Eur. J.* **2004**, *10*, 3197.
(8) Massalski, T. B. *Binary Alloy Phase Diagrams*, 2nd ed.; ASM International: Materials Park, OH, 1990; Vol. 1, p 484, Vol. 2, p 1856.
(9) (a) Pagliuso, P. G.; Sarrao, J. L.; Thompson, J. D.; Hundley, M. F.; Sercheli, M. S.; Urbano, R. R.; Rettori, C.; Fisk, Z.; Oseroff, S. B. *Phys. Rev. B*, **2001,** *63*, No. 092406-1. (b) Zaremba, V. I.; Kalychak, Y. M.; Tyvanchuk, Y. B.; Hoffmann, R.-D.; Möller, M. H.; Pöttgen, R. *Z. Naturforsch. B* **2002**, *57*, 791. (c) Macaluso, R. T.; Sarrao, J. L.; Pagliuso, P. G.; Moreno, N. O.; Goodrich, R. G.; Browne, D. A.; Fronczek, F. R.; Chan, J. Y. *J. Solid State Chem.* **2002**, *166*, 245.

10.1021/ic050941i CCC: $30.25
Published on Web 10/25/2005

flux.[11] Here, we extend this research to include other transition metals and describe the $RE_2Zn_3Ge_6$ (RE = La, Ce, Pr, Nd) phases. A number of RE/Zn/Ge compounds have been reported, including $RE_4Zn_5Ge_6$[12a] (RE = Nd, Ce, Gd), $Yb_2Zn_3Ge_3$,[12b] EuZnGe,[13] $Nd_2Zn_{15}Ge_2$,[14] $GdZn_{1.6}Ge_{0.4}$, $RE_2Zn_6Ge_3$ (RE = La, Ce, Pr, Nd, Sm, Gd),[15] and $Gd_4Zn_8Ge_{10.82}$.[16] There have been considerably more examples of alkali and alkaline earth (AE) metal Zn/Ge ternary compounds reported, including Cs_6ZnGe_8,[17] trigonal Li_2ZnGe,[18] and cubic Li_2ZnGe,[19] and hexagonal LiZnGe[20] and SrZnGe,[21] both of which have the AlB_2 structure. There are also several reported AE/ Zn/ Ge ternaries that crystallize with the $ThCr_2Si_2$ structure type, specifically, $SrZn_2Ge_2$[22] and $CaZn_2Ge_2$,[23] as well as the cubic clathrate $Ba_8Zn_8Ge_{38}$.[24]

The bonding of many of these compounds can be rationalized using the Zintl concept by assuming complete transfer of the valence electrons of the alkali, AE, RE metal, and Zn to the Ge atoms.[25] In $RE_4Zn_5Ge_6$, the structure is composed of 4 Ge atoms which are tetrahedrally coordinated by Zn and a pair of Ge dimers giving the charge balancing $(RE^{3+})_4(Zn^{2+})_5(1b-Ge^{3-})_2(Ge^{4-})_4$. Cs_6ZnGe_8 is composed of 2 deltahedra ($3b\text{-}Ge_4^{4-}$) linked by a central Zn^{2+} ion resulting in isolated $(ZnGe_8)^{6-}$ anions.

The title compounds add to the growing list of "borderline" compounds containing late transition metals with more electropositive elements, such as alkaline or rare earth metals, and electronegative main group elements, where the bonding can be rationalized with the Zintl concept, but they still display semimetallic to metallic behavior. Previous examples include $Yb_9Zn_4Bi_9$,[26] $Yb_9Zn_{4+x}Sb_9$,[27] $AE(Yb)_{14}MnPn_{11}$ (AE = Ca, Sr, Ba, Pn = Sb, Bi),[28] $Yb_{14}ZnSb_9$,[29] and KNa_3In_9.[30] Here, we describe the series of compounds, $RE_2Zn_3Ge_6$, (RE = La, Ce, Pr, Nd) whose bonding and physical properties are intermediate between classical Zintl phases and intermetallic compounds. The crystal structure, electronic band structure calculations, and magnetic and spectroscopic measurements are presented.

Experimental Section

Reagents. The following reagents were used as received without purification and were stored and handled under an N_2 atmosphere in a drybox: La (~40 mesh powder, 99.9%, Cerac, Milwaukee, WI), Ce (~250 mesh powder, 99.9%, Research Chemicals, Phoenix, AZ), Pr (~250 mesh powder, 99.9%, Research Chemicals, Phoenix, AZ), Nd (~250 mesh powder, 99.9%, Research Chemicals, Phoenix, AZ), Zn (~30 mesh granular, 99.8%, J. T. Baker Chemicals, Phillipsburg, NJ), Ge (3−5 mm shards, 99.999%, Plasmaterials, Livermore, CA), and In (3−5 mm teardrops, 99.95%, Cerac, Milwaukee, WI).

Synthesis. Method A. $RE_2Zn_3Ge_6$ (RE = La, Ce, Pr, Nd) was produced by combining 2 mmol of the rare earth element, 3 mmol of Zn, 6 mmol of Ge, and 20 mmol of In in an alumina tube which was then flame sealed in a silica tube under a reduced pressure of 10^{-4} mbar. The mixture was then heated to 1000 °C over 12 h, held for 4 h, and then ramped down to 850 °C over 2 h. The reaction was then kept at this temperature for an additional 48 h, before it was cooled to room temperature over 24 h. The majority of the In flux was removed by centrifuging the sample and filtering the molten In through a coarse filter. Indium metal tended to wet the product so further purification was carried out by chemically etching away In with acetic acid. The yields from these reactions were rather poor (about 30% based on the rare earth). Purity and crystal quality were also quite poor.

Method B. $RE_2Zn_3Ge_6$ (RE = La, Ce, Pr, Nd) was synthesized by combining 2 mmol of the rare earth element, 3 mmol of Zn, and 6 mmol of Ge and cold pressing them into a pellet. The pellet was then flame-sealed in a 13 mm fused silica tube with a carbon-coated interior under vacuum. The pellets were then heated to 790 °C for the La analogue, 780 °C for $Ce_2Zn_3Ge_6$, and 770 °C for the Pr and Nd compounds over the course of 8 h. The reaction mixtures were held at their respective temperatures for 72 h; then they were cooled to room temperature over 8 h. The reactions could also be quenched without affecting purity or crystal quality. All compounds could be made as single phases in quantitative yield by this method.

X-ray Crystallography. Single-crystal X-ray diffraction data were collected at room temperature using a Bruker AXS SMART CCD diffractometer with graphite monochromatized Mo Kα (λ = 0.71073 Å) radiation. Unit cell refinement and data merging were done with the SAINT program, and an empirical absorption correction was applied using SADABS.[31] An inspection of the systematic absences immediately showed the structure to be *C* centered. The (*hkl*) condition, $h + k = 2n$, and (*h*0*l*) *h*, $l = 2n$, were the only independent conditions found, which lead to 2

(10) (a) Rodewald, U. Ch.; Zaremba, V. I.; Galadzhun, Y. V.; Hoffmann, R.-D.; Pöttgen, R. *Z. Anorg. Allg. Chem.* **2002**, *628*, 2293. (b) Moshopoulou, E. G.; Fisk, Z.; Sarrao, J. L.; Thompson, J. D. *J. Solid State Chem*. **2001**, *158*, 25. (c) Zaremba, V. I.; Kalychak, Ya. M.; Dubenskiy, V. P.; Hoffmann, R.-D.; Rodewald, U. Ch.; Pöttgen, R. *J. Solid State Chem*. **2002,** *169*, 118.

(11) Salvador, J. R.; Gour, J. R.; Bilc, D.; Mahanti, S. D.; Kanatztidis, M. G. *Inorg. Chem.* **2004**, *43*, 1403.

(12) (a) Kranenberg, C.; Johrendt, D.; Mewis, A. *Z. Anorg. Allg. Chem.* **2001**, *627*, 539. (b) Grytsiv, A.; Kaczorowski, D.; Rogl, P.; Tran, V.; Godart, C.; Gofryk, K.; Giester, G. *J. Phys. Cond. Mater.* **2005**, *17*, 385.

(13) Pöttgen, R. *Z. Naturforsch. B* **1995**, *210*, 924.

(14) Demchenko, P.; Bodak, O. *Pol. J. Chem.* **2001**, *75*, 153.

(15) Grytsiv, A.; Bauer, E.; Berger, S.; Hilscher, G.; Michor, H.; Paul, C.; Rogl, P.; Daoud-Aladine, A.; Keller, L.; Roisnel, T.; Noel, H. *J. Phys.: Condens. Matter* **2003**, *15*, 3053.

(16) Demchenco, P.; Bodak, O.; Muratova, L. *J. Alloys Compnd.* **2002**, *339*, 100.

(17) Queneau, V.; Sevov, S. *J. Am. Chem. Soc.* **1997**, *119*, 8109.

(18) Cullman, H. O.; Hinterkeuser, H. W.; Schuster, H. U. *Z. Naturforsch. B* **1981**, *36*, 917.

(19) Schönemann, H.; Schuster, H. U. *Rev. Chim. Min.* **1976**, *13*, 32.

(20) Sportouch, S.; Belin, C.; Tillard-Charbonnel, M.; Rovira, M. C.; Canadell, E. *New J. Chem.* **1995**, *19*, 243.

(21) Rieger, W.; Parthé, E. *Monatsh. Chem.* **1969**, *100*, 439.

(22) Dörrscheidt, W.; Niess, N.; Schäfer, H. *Z. Naturforsch. B* **1976**, *31*, 890.

(23) Eisenmann, B.; May, N.; Müller, W.; Schäfer, H.; Weiss, A.; Winter, J.; Ziegleder, G. *Z. Naturforsch. B* **1970**, *25*, 1350.

(24) Kuhl, B.; Czybulka, A.; Schuster, H. U. *Z. Anorg. Allg. Chem.* **1995**, *621*, 1.

(25) Kauzlarich, S. M. *Chemistry, Structure, and Bonding of Zintl Phases and Ions;* Kauzlarich, S. M., ed.; VCH Publishers: New York, 1996; p 245.

(26) Kim, S. J.; Bilc, D.; Mahanti, S. D.; Kanatztidis, M. G. *J. Am. Chem. Soc*. **2001**, *123*, 12704.

(27) Bobev, S.; Thomspon, J. D.; Sarrao, J. L.; Olmstead, M. M.; Hope, H.; Kauzlarich, S. M. *Inorg. Chem.* **2004**, *43*, 5044.

(28) (a) Kuromoto, T. Y.; Kauzlarich, S. M.; Webb, D. J. *Chem. Mater.* **1992**, *4*, 435. (b) Chan, J. Y.; Olmstead, M. M.; Kauzlarich, S. M.; Webb, D. J. *Chem. Mater*. **1998**, *10*, 3583.

(29) Fisher, I. R.; Bud'ko, S. L.; Song, C.; Canfield, P. C.; Ozawa, T. C.; Kauzlarich, S. M. *Phys. Rev. Lett.* **2000**, *85*, 1120.

(30) Li, B.; Corbett, J. D. *Inorg. Chem.* **2002**, *41*, 3944.

Table 1. Crystallographic Data for $RE_2Zn_3Ge_6$ (RE = La, Ce, Pr, Nd)

empirical formula	$La_2Zn_3Ge_6$	$Ce_2Zn_3Ge_6$	$Pr_3Zn_3Ge_6$	$Nd_2Zn_3Ge_6$
fw	909.48	911.89	913.47	920.36
cryst syst	orthorhombic	orthorhombic	orthorhombic	orthorhombic
space group	*Cmcm*	*Cmcm*	*Cmcm*	*Cmcm*
a (Å)	5.9691(9)	5.9503(5)	5.938(2)	5.9094(7)
b (Å)	24.987(4)	24.761(2)	24.708(8)	24.619(3)
c (Å)	5.9575(9)	5.9477(5)	5.936(2)	5.9063(5)
V (Å)/*Z*	888.6(2)/4	876.31(13)/4	870.9(5)/4	859.28(17)/4
D_{calcd} (g/cm^3)	6.798	6.921	6.966	7.113
abs coeff (mm^{-1})	37.208	38.370	39.341	40.602
index ranges	$-7 \le h \le 7$	$-7 \le h \le 7$	$-7 \le h \le 7$	$-7 \le h \le 7$
	$-31 \le k \le 32$	$-32 \le k \le 31$	$-31 \le k \le 32$	$-31 \le k \le 31$
	$-7 \le l \le 7$	$-7 \le l \le 7$	$-7 \le l \le 7$	$-7 \le l \le 7$
reflns collected/unique/*R*(int)	4233/591/0.0601	4141/612/0.037	4187/614/0.038	3786/605/0.075
data/params	591/36	612/36	614/36	605/36
GOF on F^2	1.183	1.343	1.307	1.136
final R indices [$I > 2\sigma(I)$] (R1/wR2)[a]	0.0257/0.0741	0.0254/0.0719	0.0266/0.0697	0.0481/01277
R indices (all data) (R1/wR2)[a]	0.0270/0.0748	0.0261/0.0723	0.0281/0.0703	0.0492/0.1287

[a] $R1 = \sum||F_o| - |F_c||/\sum|F_o|$. $wR2 = [\sum(|F_o^2 - F_c^2|)^2/\sum(wF_o^2)^2]^{1/2}$.

possible space groups, $Cmc2_1$, and *Cmcm*.[32] The mean $|E^2 - 1|$ value of 0.912 pointed to the likelihood of a centrosymmetric space group as the estimated $|E^2 - 1|$ value for a noncentrosymmetric space group is 0.736 and for a centrosymmetric group it is 0.968. A structural solution in the *Cmcm* space group was obtained for $La_2Zn_3Ge_6$ by direct methods using the program SHELXS, and the final refinement was completed with the SHELXL suite of programs.[33] The refinements of the Ce, Pr, and Nd analogues were accomplished using the solution of $La_2Zn_3Ge_6$ as a starting point.

Data collection and refinement details for $RE_2Zn_3Ge_6$ (RE = La, Ce, Pr, Nd) are given in Table 1. Atomic coordinates and isotropic displacement parameters for all compounds can be found in Table 2. All compounds were refined with atomic positions fully occupied and without the introduction of disorder. Care was taken in the assignment of the Zn and Ge atoms in the crystal structure as their scattering factors differ by only 10%.[32] The structure we propose here gives the most reasonable bond distances, minimizes R1, wR2, and the residual electron density, and is in agreement with the elemental analysis.

Phase identity and purity were confirmed by powder X-ray diffraction carried out on an INEL diffractometer with Cu Kα radiation. The experimental powder patterns were compared to calculated powder patterns generated from the single-crystal structural refinements. Powder patterns were calculated with the CERIUS^2 software package.[34]

Elemental Analysis. Semiquantitative microprobe elemental analysis was performed on several single crystals of each of the analogues, including the crystals used for X-ray diffraction. Spectra were collected on a JEOL JSM 35C scanning electron microscope equipped with a Noran energy-dispersive spectrometer (EDS) with the Norvar window. Spectra were collected with an accelerating voltage of 20 kV and 200 s acquisition times. Standardless quantitation for these compounds led to the following atomic ratios: 1/1.25/2.75 for La, Zn, and Ge, respectively. This ratio is in reasonably good agreement with the stoichiometric ratios obtained from the crystallographic refinement. Similar stoichiometric ratios were determined for the other analogues as well.

Table 2. Atomic Coordinates ($\times 10^4$) and Equivalent Isotropic Displacement Parameters ($\times 10^3$ Å^2) for $RE_2Zn_3Ge_6$ (RE = La, Ce, Pr, Nd)

atom	Wyckoff	*x*	*y*	*z*	*U*(eq)[a]
La(1)	4c	5000	1062(1)	2500	7(1)
La(2)	4c	0	1063(1)	7500	7(1)
Ge(1)	16h	2146(1)	2021(1)	356(1)	12(1)
Ge(2)	4c	0	664(1)	2500	9(1)
Ge(3)	4c	5000	595(1)	7500	8(1)
Zn(1)	4c	5000	1616(1)	7500	12(1)
Zn(2)	8e	2407(2)	0	0	9(1)
Ce(1)	4c	5000	1065(1)	2500	6(1)
Ce(2)	4c	0	1067(1)	7500	6(1)
Ge(1)	16h	2139(1)	2016(1)	360(1)	9(1)
Ge(2)	4c	0	683(1)	2500	8(1)
Ge(3)	4c	5000	590(1)	7500	7(1)
Zn(1)	4c	5000	1612(1)	7500	11(1)
Zn(2)	8e	2381(2)	0	0	10(1)
Pr(1)	4c	5000	1065(1)	2500	6(1)
Pr(2)	4c	0	1067(1)	7500	6(1)
Ge(1)	16h	2142(1)	2014(1)	357(1)	9(1)
Ge(2)	4c	0	693(1)	2500	8(1)
Ge(3)	4c	5000	590(1)	7500	7(1)
Zn(1)	4c	5000	1606(1)	7500	10(1)
Zn(2)	8e	2371(2)	0	0	10(1)
Nd(1)	4c	0	1066(1)	2500	6(1)
Nd(2)	4c	5000	1068(1)	7500	6(1)
Ge(1)	16h	2852(2)	2013(1)	351(2)	9(1)
Ge(2)	4c	5000	699(1)	2500	7(1)
Ge(3)	4c	0	593(1)	7500	7(1)
Zn(1)	4c	0	1604(1)	7500	10(1)
Zn(2)	8e	2371(2)	0	0	9(1)

[a] *U*(eq) is defined as one-third of the trace of the orthogonalized U^{ij} tensor.

Differential Thermal Analysis. Differential thermal analysis (DTA) was carried out with a Shimadzu DTA-50. Samples were flame sealed under a reduced atmosphere in fused silica ampules that were carbon coated to prevent glass attack upon melting of the products. An α-Al_2O_3 standard was used as a reference. The analysis was done by heating the sample at a rate of 10 °C per minute up to 1000 °C, then cooling to 150 °C at the same rate, and then repeating the cycle. To determine an appropriate reaction temperature for $RE_2Zn_3Ge_6$, we carried out 0.1 mmol scale reactions in the DTA instrument. Reactants were combined in their stoichiometric ratios and heated to 1000 °C at 10 °C/min and then cooled to 150 °C at the same rate, in an attempt to determine at what temperature the reaction takes place.

(31) (a) *SAINT*, version 5; Siemens Analytical X-ray Instruments, Inc.: Madison WI, 1995. (b) Sheldrick, G. M. *SADABS*; University of Göttingen: Göttingen, Germany, 1997.
(32) Hahn, T. *International Tables For Crystallography*, 4th ed.; Kluwer Academic: Boston, 1987; Vol. B, pp 45, 314−315.
(33) Sheldrick, G. M. *SHELXTL. Structure Determination Program*, version 7.0; Siemens Analytical X-ray Instruments, Inc.: Madison, WI, 1997.
(34) *CERIUS^2*, version 1.6; Molecular Simulations Inc.: Cambridge, U.K., 1994.

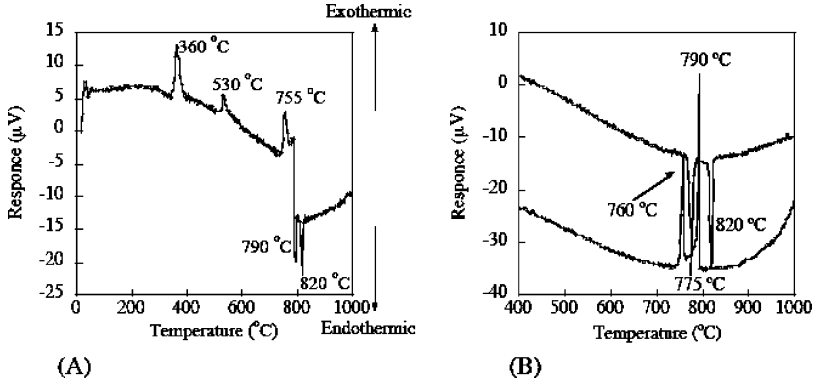

Figure 1. (A) Initial heating cycle for a mixture of La/Zn/Ge in the differential thermal analyzer. There are 3 exothermic peaks in the first heating cycle at 360, 530, and 755 °C. The endotherm at 790 °C is thought to correspond to the reaction forming $La_2Zn_3Ge_6$, and the endothermic peak at 820 °C is thought to correspond to its melting point. (B) The second heating cycle of the now reacted elements. The endotherm at 775 °C is the melting point of an impurity from the incongruent melting of $La_2Zn_3Ge_6$ in the first heating cycle.

Magnetic Susceptibility Measurements. The magnetic susceptibility measurements were carried out on a Quantum Design MPMS SQUID magnetometer. Measurements were performed on polycrystalline samples that were placed in an envelope made of Kapton tape. Magnetic susceptibility data were collected in both field-cooled and zero-field-cooled modes with an applied field of 500 Oe for the La, Ce, and Nd analogues and 2000 Oe for $Pr_2Zn_3Ge_6$ between 2 and 300 K. Magnetization data were collected at 2 K with fields sweeping from −55 kOe to 55 kOe. A correction was applied to the raw susceptibility data to account for the diamagnetic contributions of the core electrons[35] and the sample container.

Diffuse-Reflectance Infrared Spectroscopy. Band-gap energy measurements were carried out by diffuse-reflectance infrared spectroscopy. Reflectance data were converted to absorption using the Kubelka−Munk equation.[36] The measurements were performed on a Nicolet Magna750 Fourier transform infrared spectrometer.

Band Structure Calculations. Band structure calculations were performed on $La_2Zn_3Ge_6$ using the self-consistent full-potential linearized augmented plane wave method (LAPW)[37] within density functional theory (DFT), with a generalized gradient approximation (GGA) for the exchange and correlation potential within the Perdew−Burke−Ernzerhof model.[38] Scalar relativistic corrections were added and spin−orbit interactions (SOI) were incorporated using a second variational procedure.[39] Calculations were carried out on the La system because of the inability of DFT to accurately model the highly correlated electrons found in partially filled *f* levels. The calculations were performed with the WIEN2K program.[40] The atomic radii values (in atomic units 1 au = 0.529 Å) used in the calculation are as follows 2.4 for La, 2.15 for Zn, and 2.25 for Ge. Self-consistent iterations were performed with 27 *k* points in the reduced Brillouin zone with a cutoff between valence and core states of −6.0 Ry; convergence was assumed when the energy difference between cycles was less than 0.0001 Ry.

(35) Selwood, P. W. *Magnetochemistry*, 2nd ed.; Interscience Publishers: New York, 1956; p 70.
(36) (a) Wendlandt, W. W.; Hecht, H. G. *Reflectance Spectroscopy*; Interscience Publishers: New York, 1966. (b) Tandon, S. P.; Gupta, J. P. *Phys. Status Solidi* **1970**, *38*, 363.
(37) (a) Hohenberg, H.; Kohn, W. *Phys. Rev.* **1964**, *136*, B864. (b) Kohn, W.; Sham, L. *Phys. Rev.* **1965**, *140*, A1133. (c) Singh, D. *Planewaves, Pseudopotentials, and the LAPW Method*; Kluwer Academic: Boston, 1994.
(38) Perdew, J. P.; Burke, K.; Ernzerhof, M. *Phys. Rev. Lett.* **1996**, *77*, 3865.
(39) Koelling, D. D.; Harmon, B. *J. Phys. C* **1980**, *136*, 147.
(40) Blaha, P.; Schwarz, K.; Luitz, J. *WIEN97, A Full Potential Linearized Augmented Plane Wave Package for Calculating Crystal Properties*; Universität Wien: Vienna, Austria, 2000.

Results and Discussion

Synthesis and Stability. The title compounds were originally found in an indium flux reaction of the elements with the stoichiometric ratio 1/1/3/20 for La, Zn, Ge, and In, respectively. The crystals of $La_2Zn_3Ge_6$ were stable in glacial acetic acid, water, and acetone but were of poor quality. When the reactants were combined in their stoichiometric ratios for the In flux reactions, the yields were still generally poor. The crystals grew as stacks of very thin plates that could not be easily mechanically separated. A crystal from this method was used for single-crystal X-ray diffraction, but the quality of data was poor with very large standard deviations in the lattice parameters and large residual electron densities. The best crystals for X-ray diffraction came from direct combination reactions.

Several attempts to make these compounds by direct combination of the elements employing arc melting or a radio frequency induction furnace did not work because of the large vapor pressure of molten Zn. Reactions were also carried out in conventional furnaces by heating the reactants to 1000 °C and holding for 72 h, before quenching the reactions to room temperature. These reactions were successful in producing the target compound, but the products had multiple phases. It was found, however, that shorter heating times of 24 to 48 h tended to improve phase purity. Lower reaction temperatures of 850 °C and 750 °C with reaction times of 72 h also produced multiphase samples. When reactions were carried out at 850 °C, the target phase, $RE_2Zn_3Ge_6$, dominated the mixture, while reactions heated at 750 °C yielded a RE/Ge binary and re-crystallized Zn with no sign of the target phase in the product powder pattern.

To find a temperature that was appropriate for running these reactions, we combined the elements in their stoichiometric ratio on the 0.1 mmol scale for a small trial reaction in a DTA. The reactants were then heated to 1000 °C at a rate of 10 °C/min. The DTA experiments for a stoichiometric mixture of La/Zn/Ge showed three exothermic events in the first heating cycle at 360, 530, and 755 °C followed by 2 endothermic events at 790 and 820 °C (Figure 1A). When the sample was heated again from room temperature to 1000 °C, two melting peaks were found at 775 and 820 °C, and

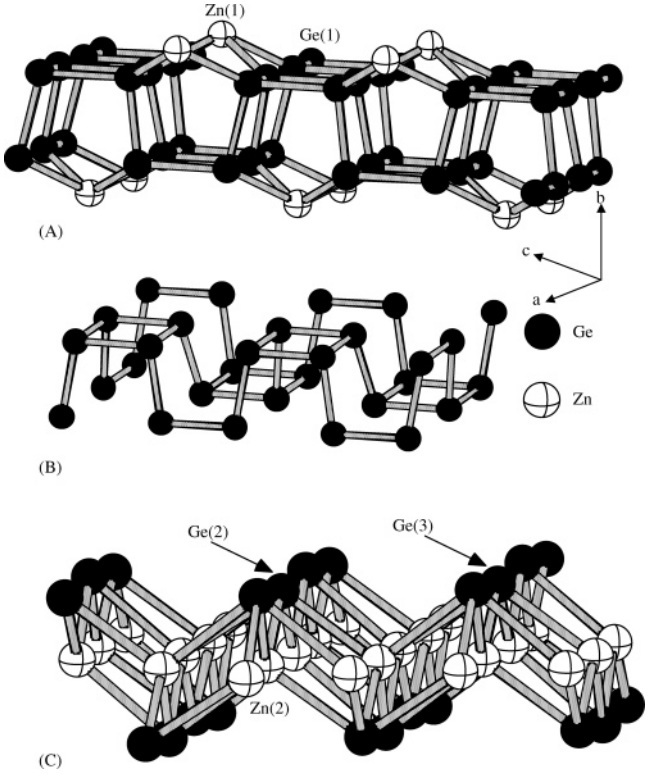

Figure 2. (A) View of the pentagonal $ZnGe_4$ cage structure which extends in the *ac* plane and is similar to those found in $Sm_2Ni(Ni_xSi_{1-x})Al_4Si_{6-y}$ and $Ce_4Zn_8Ge_{11-x}$. (B) Perspective view of the Ge^{-1} fragment. (C) View of the ZnGe PbO-type layer, which extends in the *ac* plane.

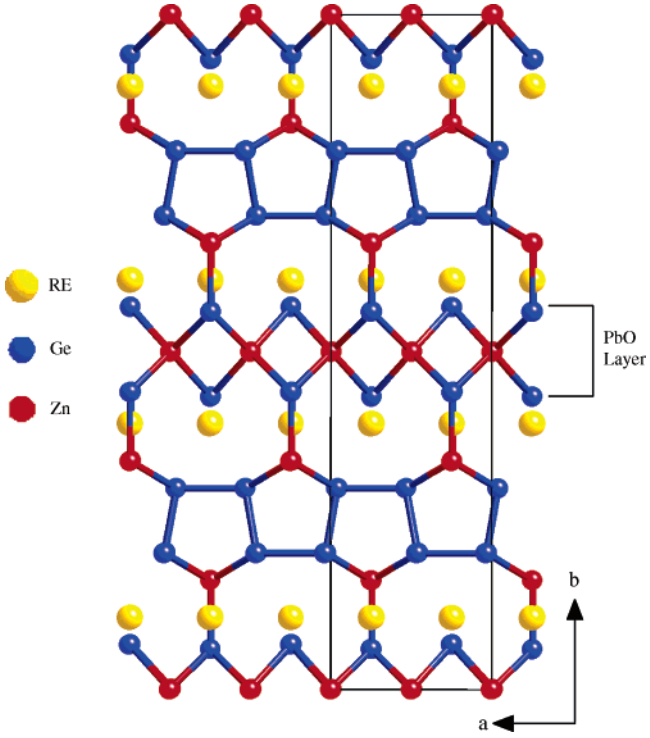

Figure 3. Structure of $RE_2Zn_3Ge_6$ as viewed along the *c* axis.

upon cooling, two recrystallization peaks at 790 and 760 °C were also found (Figure 1B).

Powder patterns taken after the initial heating cycle and after the second heating cycle showed that the samples were both multiphasic with $La_2Zn_3Ge_6$ being dominant. Similar results were obtained for other rare earth metal analogues. The endothermic peak at 790 °C did not reappear in the second cycle of heating, neither did any of the exothermic peaks that were found upon heating. We therefore inferred that the formation of the target phase was taking place around 790 °C since the reactions did not yield the target phase when heated at or below 750 °C.

As a result of these studies, all $RE_2Zn_3Ge_6$ could be made as pure phases in quantitative yield by pressing a pellet of the reactants in their stoichiometric ratios and heating them for 72 h at 790 °C for La, 780 °C for Ce, and 770 °C for the Nd and Pr reactions. The DTA experiments provided insight as to why the other reaction conditions could not yield a pure phase. Originally, the reactions were being carried out above the melting point of the product, and because it melts incongruently, impurity phases were formed; the reactions at 750 °C were not sufficiently warm to form the target phase over the period of 3 days.

Structure. $RE_2Zn_3Ge_6$ (RE = La, Ce, Pr, Nd) compounds crystallize in the orthorhombic C*mcm* space group and are composed of two types of slabs which alternately stack along the *b* axis with the rare earth atoms located between the layers. The first building unit is a $ZnGe_4$ layer (Figure 2A). This slab is composed of 4 atomic layers in the order Zn(1), Ge(1), Ge(1), and Zn(1). If the square pyramidal coordinated Zn(1) atoms are removed, the remaining Ge fragment becomes an infinite, puckered layer composed of interconnected squares (Figure 2B). This is an unusual arrangement for Ge atoms with only two previous reports of its occurrence: one is in the tetragonal structure $Sm_2Ni(Ni_xGe_{1-x})Al_4Ge_6$, [41] which is the Ge analogue of the previously reported Si-containing compound,[42] and the other is the tetragonal (*P*4/*nmm*) $Ce_4Zn_8Ge_{10.82}$,[42] whose structure was elucidated by single-crystal X-ray diffraction and bears a striking resemblance to the title compounds. Using the Zintl concept, this fragment can be thought of as being composed of Ge^{1-} atoms, as each Ge is bound to three other Ge atoms thus requiring 1 extra electron to fill its octet (i.e., isoelectronic to phosphorus) (Figure 2B). The Zn(1) atom makes 4 bonds to Ge forming the bridging units which join the distorted square nets (Figure 2A). The result is a layer of intersecting pentagonal channels which run along the *a* and *c* axes.

The second building unit in $RE_2Zn_3Ge_6$ is a PbO-like slab composed of Zn and Ge with Zn occupying the O sites and Ge the Pb sites (Figure 2C). This layer and the $ZnGe_4$ layer extend in the *ac* plane and are interconnected along the *b* axis through a Ge(3)−Zn(1) bond as shown in Figure 3. The Zn_2Ge_2 layer is composed of 2 crystallographically distinct Ge atoms and a Zn atom. The Zn(2) atoms are tetrahedrally coordinated by 2 Ge(2) atoms and 2 Ge(3) atoms. The resulting structure of the title compounds can be charge balanced as follows: $(La^{3+})_2(Zn^{2+})_3(3b\text{-}Ge^{1-})_4(Ge^{4-})_2$. A full list of bond distances for $RE_2Zn_3Ge_6$ (RE = La, Ce, Pr, Nd) are given in Table 3.

The structure of the title compound bears a striking resemblance to the $Ce_4Zn_8Ge_{11-x}$[43] structure type, of which $Gd_4Zn_8Ge_{10.82}$[16] is a member. Both crystallize in the tetragonal *P*4/*nmm* space group. $Ce_4Zn_8Ge_{11-x}$ has Ge_5 layers

Table 3. Bond Distances (Å) for $RE_2Zn_3Ge_6$ (RE = La, Ce, Pr, Nd) with Estimated Standard Deviations (esds)

		La	Ce	Pr	Nd
RE(1)−Ge(2)	2×	3.1461(6)	3.1216(5)	3.108(1)	3.0900(7)
RE(1)−Ge(3)	2×	3.1995(6)	3.1975(6)	3.192(1)	3.1745(8)
RE(1)−Ge(1)	4×	3.2047(8)	3.1727(8)	3.162(1)	3.144(1)
RE(1)−Zn(1)	2×	3.2842(7)	3.2673(7)	3.255(1)	3.237(1)
RE(1)−Zn(2)	2×	3.4147(7)	3.4050(7)	3.401(1)	3.389(1)
RE(2)−Ge(2)	2×	3.1412(6)	3.1220(5)	3.109(1)	3.0902(7)
RE(2)−Ge(1)	4×	3.2036(8)	3.1678(8)	3.158(1)	3.139(1)
RE(2)−Ge(3)	2×	3.2052(6)	3.2007(6)	3.194(1)	3.1781(8)
RE(2)−Zn(1)	2×	3.2888(7)	3.2662(7)	3.254(1)	3.236(1)
RE(2)−Zn(2)	2×	3.3671(7)	3.3468(7)	3.337(1)	3.326(1)
Ge(1)−Ge(1)	1×	2.469(2)	2.469(1)	2.471(1)	2.473(1)
Ge(1)−Ge(1)	1×	2.555(1)	2.546(1)	2.544(2)	2.538(2)
Ge(1)−Ge(1)	1×	2.561(1)	2.546(1)	2.354(2)	2.539(2)
Ge(1)−Zn(1)	4×	2.6119(9)	2.6068(9)	2.603(1)	2.586(1)
Ge(2)−Zn(2)	4×	2.6528(9)	2.661 (1)	2.667(1)	2.665(1)
Ge(3)−Zn(1)	1×	2.550(2)	2.528(2)	2.511(2)	2.490(3)
Ge(3)−Zn(2)	2×	2.6124(9)	2.6034(9)	2.601(1)	2.593(1)

isostructural to the $ZnGe_4$ layers of the title compound and also has Zn layers isostructural to the ZnGe−PbO layers. The Zn−Zn distances in the structure of $Ce_4Zn_8Ge_{11-x}$ are unreasonably close (2.54 Å in the Zn PbO-like layer), and the atoms are partitioned into Zn layers and Ge layers, which is highly unusual. It is likely that $Ce_4Zn_8Ge_{11-x}$ is completely isostructural to the title compounds but with a misassignment of the crystal system and atomic positions. These misassignments may lead to the partial occupancy of the Ge site as well as the deviation from the stoichiometry we report. Additionally, in the report of $Gd_4Zn_8Ge_{10.82}$, the structure was determined by Rietveld powder X-ray diffraction using the $Ce_4Zn_8Ge_{11-x}$ structure type as a model, and as we report, $RE_2Zn_3Ge_6$ has nearly identical cell parameters for the *a* and *c* axes; therefore, the orthorhombic lattice would be easily mistaken as tetragonal.

Band Structure Calculations. The bonding in $RE_2Zn_3Ge_6$ can be rationalized using the Zintl concept in the following manner. The rare earth ions are assumed to be in the 3+ oxidation state while the Zn ions have a filled *d* shell and the 3 *s* orbitals are assumed vacant resulting in 2+ cations. The remaining Ge atoms fulfill their octet requirements by forming bonds and by formal reduction. Specifically, Ge(1) which is tetrahedrally coordinated by 3 other Ge(1) atoms and one Zn ion would have a formal charge of −1 while the remaining Ge atoms are isolated from one another, an arrangement that requires them to adopt a formal −4 charge to fulfill octet requirements. The overall structure is then formally charge-balanced as $(RE^{3+})_2(Zn^{2+})_3(Ge^{-1})_4(Ge^{4-})_2$. The result would lead us to anticipate semiconducting behavior from these compounds.[44]

To better understand the nature and bonding in these phases and to see if a band gap could be computed, we carried out ab initio band structure calculations at the DFT level. The total density of states (DOS), as computed for $La_2Zn_3Ge_6$, can be seen in Figure 4A. There are three main features in this diagram. The first is the large narrow band located between −8 and −7 eV, which corresponds to the filled d^{10} levels of the Zn ions. This is verified by inspection of the partial DOS for the Zn d orbitals which shows only this feature (Figure 4B). The second feature is the large band located between 1 and 10 eV, which has it origins in the 5d orbitals of the La ions. Finally, the DOS at the Fermi level is small, but nonzero, at less that 5 states/eV/2[$La_2Zn_3Ge_6$]. This can be seen more clearly in the inset of Figure 4A. This finding indicates that the materials are not semiconductors as the simplistic charge-balancing would indicate but are instead semimetals.

To determine which levels contribute to the DOS at the Fermi level, we first investigated the partial DOS of each of the individual species. The 5d levels of the two crystallographically distinct La atoms were found to have significant contributions to the DOS at the Fermi level (Figure 4C). This would indicate that these levels are at least partially filled and hybridized with the Zn_3Ge_6 sublattice leading to incomplete charge transfer from the RE sublattice to the Zn_3Ge_6 one. Other orbitals which make significant contributions to the DOS at the Fermi level include the p orbitals of Ge(1), Ge(2), and Ge(3) (Figure 4D) and the s orbitals of Zn(2). There is a substantial difference in the DOS between Ge(1) and the other Ge atoms, especially in the number of states at the Fermi level where Ge(1) is significantly larger.

Fat-band analysis (the radius of the circles that trace out the various bands is proportional to the contribution from that particular state) of the band structure was done to determine which of these bands cross the Fermi level and in which direction in the Brillouin zone they cross it. Figure 5A shows the geometry and special directions for a C-centered orthorhombic Brillouin zone. Figure 5B shows the p-orbital contribution to the band structure for Ge(1) which is involved heavily in bands that cut across the Fermi level along the YT ((0,1/2,0) to (0, 1/2, 1/2)), and the ZΓ ((0,0,1/2) to (0,0,0)) directions. These p orbitals also contribute to the conduction band which dips below the Fermi level around the R Brillouin zone point (1/4, 1/4, 1/2).

Both Ge(2) and Ge(3) make very strong contributions to the bands along the ΓY direction ((0,0,0) to (0,1/2,0)), as well and the YT ((0,1/2,0) to (0,1/2,1/2)), ZΓ, and ΓR directions (Figure 5C). The ΓY direction coincides with the axis along which $ZnGe_4$ and Zn_2Ge_2 stack. The YT section, which is parallel to the slabs, shows a strong contribution from Ge(2) and Ge(3) with a conduction-band crossing of these orbitals along this axis. Other conduction-band crossings involving these orbitals take place along the ΓZ and ΓΣ ((0,0,0) to (1/4,0,0)), both of which are again parallel to the Zn/Ge slabs. The Ge(2) and Ge(3) p orbitals contribute to bands that also have rather strong contributions from

(41) Sieve, B. J. Exploratory Synthesis of Quaternary Rare Earth Transition Metal Aluminum Tetralides: Utilizing Molten Al as a Solvent. Ph.D. Dissertation, Michigan State University, East Lansing, MI, 2002, Chapter 4.

(42) Chen, X.-Z.; Sportouch, S.; Sieve, B.; Brazis, P.; Kannewurf, C. R.; Cowen, J. A.; Patschke, R.; Kanatzidis, M. G. *Chem. Mater.* **1998**, *10*, 3202.

(43) Opainych, I. M. Ph.D. Thesis, Department of Inorganic Chemistry, L'viv State University, L'viv, Ukraine, 1996.

(44) Diffuse reflectance infrared spectra were collected in the range of 0.1−0.5 eV for each of the analogues, and in each case, no band gap was detected. If there is a gap, which is contrary to the band structure calculations, it is likely to be <0.1 eV which is beyond the capability of our instrument.

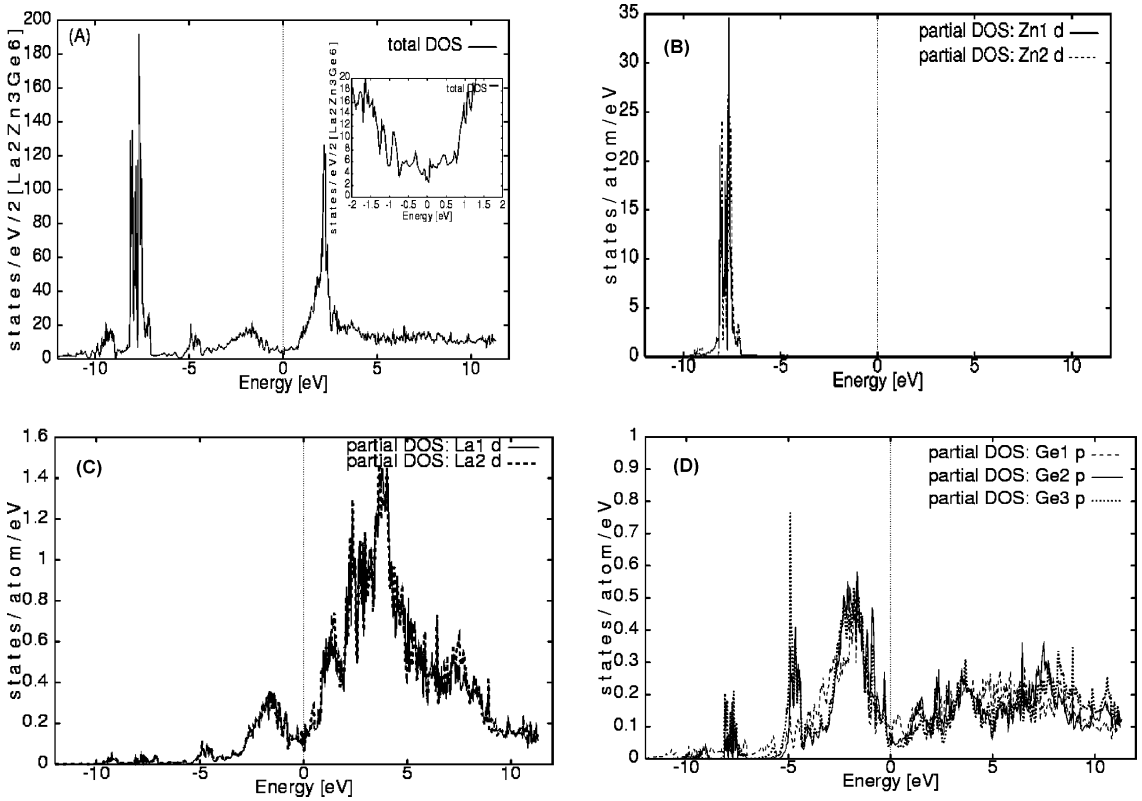

Figure 4. (A) Total density of states (DOS) for $La_2Zn_3Ge_6$. The inset shows a close-up view illustrating the low DOS at the Fermi level characteristic of a semimetal. (B) The partial DOS for the Zn d electrons showing them well below the Fermi level. (C) The partial DOS for the La d electrons distributed above and below the Fermi level. (D) The partial DOS for the Ge p electrons showing them mainly above the Fermi level.

Zn(2) s orbitals and also cross the Fermi level suggesting that they hybridize by lowering the energy of the Zn s orbitals below the Fermi level (Figure 5D) leading to negative band gaps.

The d orbitals of La(1) and La(2) make strong contributions to bands crossing the Fermi level in virtually every direction in the Brillouin zone, as shown in Figure 5E and F for La(1) and La(2), respectively. This is consistent with their partially filled character indicated by the DOS. These orbitals hybridize quite strongly with Ge(2) and Ge(3) along the ΓY, YT, ΓZ, and ΓR. There is also significant hybridization of these d states with the Ge(1) p orbitals in the YT, ΓR ((0,0,0) to (1/4, 1/4, 1/2)), and RS ((1/4, 1/4, 1/2) to ((1/4, 1/4, 0)) directions.

The conduction bands which cross the Fermi level are composed of Ge p, La d, and Zn(2) s orbitals. This likely results from the fact that there is orbital overlap and incomplete electron transfer from the putative Zn^{2+} to Ge^{4-} within the Zn_2Ge_2 layer and between the La ions and the Zn_3Ge_6 sublattice. This results in the lowering of the Zn s and La d states allowing them to hybridize with the Ge(2) and Ge(3) p states contributing to the negative band gaps we observe in the band structure.

The Zn(1) s orbitals do not make appreciable contribution to any bands that cross the Fermi energy, instead the p orbitals of these atoms hybridize with the p states of Ge(1). These interactions likely push the p levels above the Fermi level along YT and the ΓZ for both Ge(1) and Zn(1). As with the Zn_2Ge_2 layer, the bands with Zn(1) and Ge(1) contributions which cross the Fermi level do so parallel to the plane of the $ZnGe_4$ fragment, not perpendicular to them.

The result of this is a three-dimensional metal as the Fermi surface is crossed in all three directions indicating charge-carrier mobility in each axis. Charge transport along the *b* axis should be dominated by the Ge(2) and Ge(3) p orbitals and the La d orbitals. These bands contribute most heavily to the band that crosses the Fermi level along the ΓY direction. Ge(2) and Ge(3) p orbitals hybridize with the Zn-(2) s orbitals creating bands which cross the Fermi level parallel to the Zn_2Ge_2 layer. Likewise, in the $ZnGe_4$ layer, the Ge(1) p states hybridize with the Zn(1) p states which cross the Fermi level parallel to the layer. The d states of La are also heavily involved in charge transport parallel to the layers.

There are several examples of alkaline and rare earth metals showing incomplete electron transfer from the electropositive elements to the electronegative elements resulting in enhanced covalent interactions between these lattices as in $Ba_5In_4Bi_5$[45] and Yb_3Ga_6 Ge_4.[7] The situation found in these materials is mirrored in $RE_2Zn_3Ge_6$; we expect the early rare earth metals and Zn to behave in much the same way as the Ba and Yb ions behave in $Ba_5In_4Bi_5$ and Yb_3Ga_6 Ge_4.

Magnetic Properties. As there are two crystallographically distinct rare earth ions per formula unit, $RE_2Zn_3Ge_6$ will have an effective magnetic moment that is calculated by eq 1

$$\mu_{\text{total}} = \sqrt{\mu_{\text{eff}}^2(\text{a}) + \mu_{\text{eff}}^2(\text{b})} \qquad (1)$$

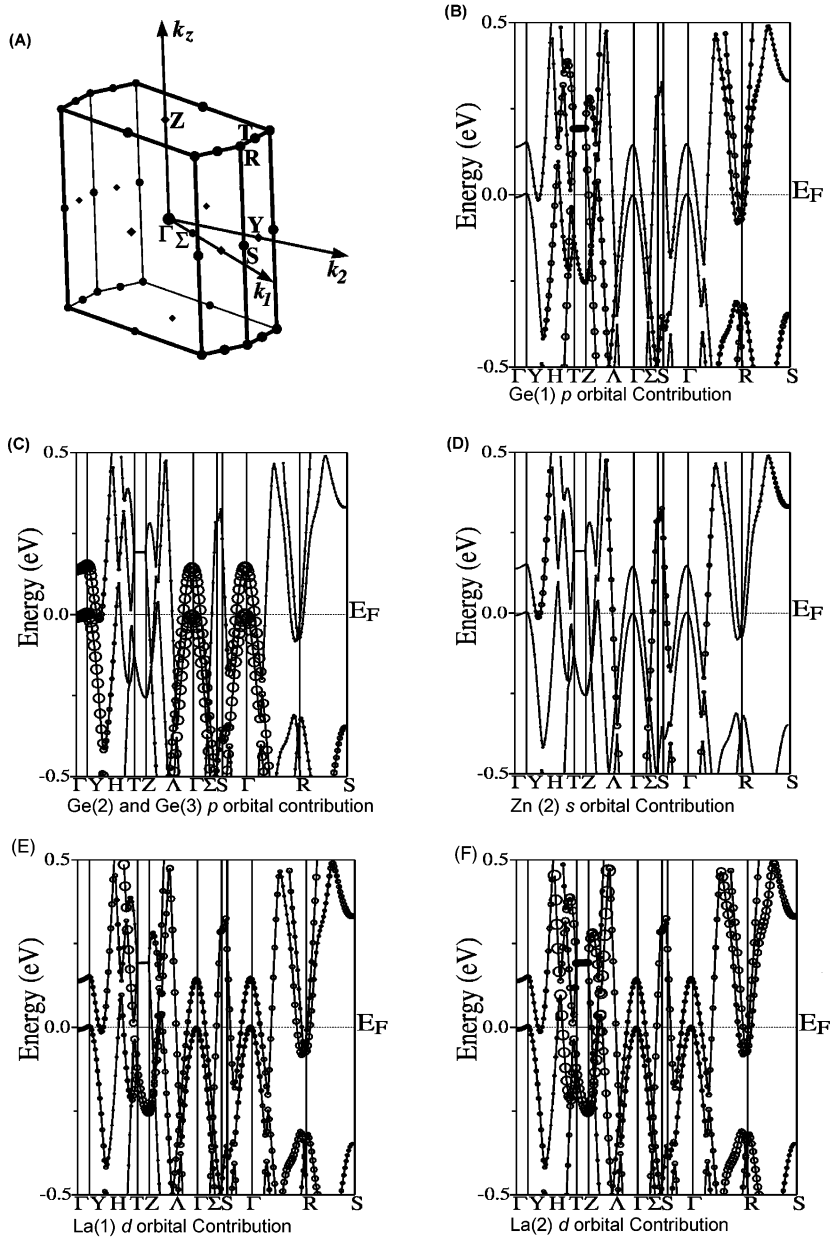

Figure 5. (A) The Brillouin zone for a C-centered orthorhombic unit cell. (B) Band structure of $La_2Zn_3Ge_6$ between −0.5 and 0.5 eV showing the Ge(1) p-orbital contribution to be bands in the vicinity of the Fermi level. In this projection, the breadth of the circles tracing out the band are proportional to the orbital's contribution. (C) The Ge(2) p-orbital contribution to the band structure. Not shown is the Ge(3) p contribution which is identical to that of Ge(2). (D) The Zn(2) s-orbital contribution to the band structure. (E) The La(1) d-orbital contribution to the band structure. (F) The La(2) d-orbital contribution to the band structure.

where μ_{total} is the effective magnetic moment per formula unit and μ_{eff}(a) and μ_{eff}(b) are the calculated effective magnetic moments of each of the two rare earth (3+) ions. On the basis of previous work with rare earth- and late transition metal-containing compounds, we expect that the only paramagnetic contribution found in these phases will be from the RE^{3+} ions.

$La_2Zn_3Ge_6$. The susceptibility for $La_2Zn_3Ge_6$ displays temperature-independent diamagnetism. This is in agreement with what we expect because the d shell for Zn is filled, as are the bands for Ge, so the only paramagnetic contribution would be expected to come from the rare earth ion, but as La is f^0, it too is diamagnetic. The fact that the susceptibility is negative implies a low DOS at the Fermi level, as systems with large DOS values typically display high Pauli paramagnetism. This type of paramagnetism is the result of polarization of the conduction electrons in a metal by the applied field. If this effect is small, as it would be in semimetals, then the core electron diamagnetism will dominate giving negative susceptibility, as observed for $La_2Zn_3Ge_6$.

$Ce_2Zn_3Ge_6$. The susceptibility data for $Ce_2Zn_3Ge_6$ obeys the Curie/Weiss law over a rather small temperature range from 5 to 200 K (Figure 6A); above this temperature, the inverse susceptibility changes slope. The region where the Curie/Weiss law was followed resulted in an effective magnetic moment of 3.71 μ_B, which is in good agreement with 3.6 μ_B, the value calculated for 2 independent Ce^{3+} ions (2.54 μ_B per Ce atom).[46] The Weiss constant is small with a

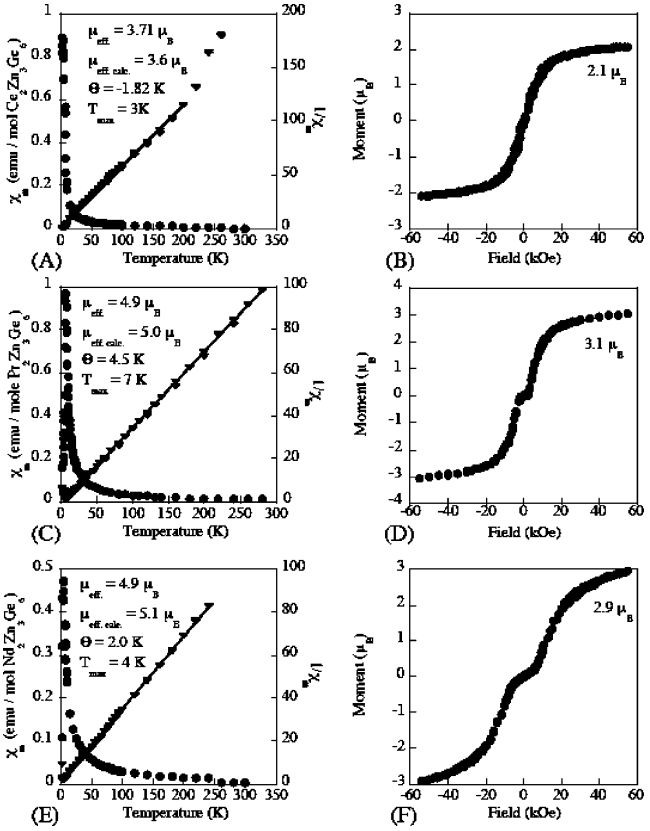

Figure 6. (A) Magnetic susceptibility for $Ce_2Zn_3Ge_6$ collected from 2 to 300 K in both field-cooled and zero-field-cooled modes. (B) Magnetization data for $Ce_2Zn_3Ge_6$ collected at 2 K. (C) Magnetic susceptibility data for $Pr_2Zn_3Ge_6$ collected from 2 to 300 K with an applied field of 2000 Oe. (D) The magnetization curve for $Pr_2Zn_3Ge_6$. (E) Magnetic susceptibility data for $Nd_2Zn_3Ge_6$ collected between 2 and 300 K with an applied field of 500 Oe. (F) Magnetization curve for $Nd_2Zn_3Ge_6$.

value of −1.8 K indicating weak anitferromagnetic interactions. The susceptibility data for $Ce_2Zn_3Ge_6$ has a maximum at 3 K suggesting that it orders antiferromagnetically at this temperature. The deviation above 200 K is likely to be the result of the crystal-field splitting of the Ce^{3+} 5/2 multiplet.[47]

The magnetization curve for $Ce_2Zn_3Ge_6$ at 5 K is given in Figure 6B. As the field is increased, there is a drastic increase in the moment. It is likely that the antiferromagnetic order is disrupted by the application of a very small field. The moment depends linearly on the field up to approximately 15 kOe, at which point it begins to saturate. Linear behavior returns at about 20 kOe, but the slope is much smaller. This trend persists up to the maximum field without full saturation. The resulting moment at the maximum field (55 kOe) is ∼2.1 μ_B, which is about 60% of the value expected.[45]

$Pr_2Zn_3Ge_6$. The susceptibility data for $Pr_2Zn_3Ge_6$ are shown in Figure 6C. This compound also exhibits a maximum in susceptibility, suggesting that it also orders antiferromagnetically. Above this temperature, the data obey a Curie/Weiss law with a measured effective magnetic moment of 4.9 μ_B, which is in reasonably good agreement with the value calculated for 2 Pr^{3+} ions which is 5.1 μ_B.[46] The Pr^{3+} ion is again, the only species that makes a paramagnetic contribution to the susceptibility indicating that the rest of the species have closed shells. The Weiss constant was determined to be 4.5 K indicating weak ferromagnetic interactions between the rare earth ions.

The magnetization curve for $Pr_2Zn_3Ge_6$ at 5 K is shown in Figure 6D. In the low-field region from 0 to 3.6 kOe, the moment has weak field dependence; however, at this point, there is a substantial increase in the moment over a narrow field range. This behavior, as in the case of $Ce_2Zn_3Ge_6$, may be the result of the magnetic field disrupting the antiferromagnetic order, and it implies metamagnetic character. Above 20 kOe, the moment begins to saturate and increases linearly with field with a small slope and reaches a value of 3.1 μ_B at 55 kOe. This is about 65% of the value expected for μ_{sat}.

$Nd_2Zn_3Ge_6$. The magnetic susceptibility data for $Nd_2Zn_3Ge_6$ can be found in Figure 6E. This compound also exhibits a maximum in the susceptibility data which again suggests that it undergoes an antiferromagnetic transition at about 4 K. Above this temperature, $Nd_2Zn_3Ge_6$ displays Curie/Weiss behavior with a measured effective magnetic moment of 4.9 μ_B which is, again, in good agreement with the calculated value of 5.12 μ_B for Nd^{3+}.[46] The Weiss constant is −2.0 K indicating weak antiferromagnetic coupling between the ions.

Figure 6F shows the magnetization data taken at 2 K for $Nd_2Zn_3Ge_6$. This compound also undergoes a transition as evidenced by the abrupt slope change at 8 kOe and also shows signs of metamagnetic behavior. This transition takes place at a considerably higher field, when compared to the Ce and Pr analogues, which have critical fields of 1 and 3.6 kOe, respectively. Above 8 kOe the moment increases rapidly with field up to 12 kOe. At this point, the slope decreases, and the moment slowly increases to the highest field attainable, reaching a value of 2.8 μ_B, which is again only 60% of the calculated saturation moment (4.6 μ_B).

The magnetic behavior for the series of compounds, $RE_2Zn_3Ge_6$ (RE = La, Ce, Pr, Nd), has several things in common. Above the susceptibility maximum, all compounds follow the Curie/Weiss law with effective magnetic moments that are consistent with 3+ RE ions. The exceptions to this are $La_2Zn_3Ge_6$, which has temperature-independent diamagnetic behavior, and the Ce analogue, which changes behavior above 200 K.

Conclusions

The family of intermetallic compounds, $RE_2Zn_3Ge_6$, has structure and bonding that can be rationalized with the Zintl concept, but they are found to be semimetallic. The semimetallic nature stems from the orbital overlap between the Zn and Ge orbitals and between the RE and Zn_3Ge_6 substructure orbitals. This leads to partial band filling and a small, but significant, density of states at the Fermi level. Because of this hybridization and the resulting semimetallic character, these compounds belong to the small class of

(45) Ponou, S.; Fässler, T. F.; Tobias, G.; Canadell, E.; Cho, A.; Sevov, S. C. *Chem. Eur. J.* **2004**, *10*, 3615.
(46) Van Vleck, J. H. *The Theory of Electronic and Magnetic Susceptibility:* Oxford University Press: London, 1932.
(47) Kittel, C. *Introduction to Solid State Physics*, 7th ed.; Wiley: New York, 1996; p 425.

materials that lie near the border between classical Zintl phases and intermetallics. The rare earth ions are in a 3+ oxidation state and make the only paramagnetic contribution to the susceptibility. These compounds are likely to be isostructural to the previously reported $Ce_4Zn_8Ge_{11-x}$, whose space group was assigned as the primitive tetragonal because of the nearly identical values of the *a* and *c* lattice parameters. The fact that these compounds could be made as pure phases with the stoichiometry we report and the nonstoichiometric phase reported previously ($Gd_4Zn_8Ge_{10.82}$) suggests that this system may have a considerable phase width ($RE_2Zn_{3+x}Ge_{6-x}$).

Acknowledgment. Financial support from the Department of Energy (Grant DE-FG02-99ER45793) and the NSF-DMR summer solid state chemistry program for J.R.G. is gratefully acknowledged. Part of this work was carried out at the Center for Advanced Microscopy and the Center for Sensor Materials at Michigan State University. M.G.K. thanks the Alexander von Humboldt Foundation for a Fellowship.

Supporting Information Available: Crystallographic data in CIF format for $La_2Zn_3Ge_6$, $Ce_2Zn_3Ge_6$, $Pr_2Zn_3Ge_6$, and $Nd_2Zn_3Ge_6$. This material is available free of charge via the Internet at http://pubs.acs.org.

IC050941I